IR Imaging of Circumstellar Environments

W.C. Danchi, P.G. Tuthill, M. Bester, E.A. Lipman, J.M. Monnier, & C.H.Townes

Space Sciences Laboratory, University of California, Berkeley, Berkeley, CA 94720-7450 USA

Abstract.

Long baseline interferometry at mid-infrared (8-12 μm) and near-infrared (J,H,K,L) bands is providing a new observational perspective on the environment within a few stellar radii of the photospheres of late-type stars. Results will be presented primarily from recent work with the University of California, Berkeley, Infrared Spatial Interferometer, a two-telescope stellar interferometer, having a variable baseline. Interferometry in the mid-infrared is particularly suited to examining the distribution of dust clouds emitted by late-type stars, and also stellar diameters, since the effects of limb-darkening and stellar hot spots are small. Results show the location of initial dust formation, the distribution of emitted material, and in some cases its motion, the average rates of emission of material, and the relation between circumstellar clouds and masers. Of the sample of 15 stars studied thus far, a substantial fraction has major dust emission episodes separated by 10-100 years; others emit continuously or on each luminosity cycle. Stars which have been studied in some detail include IRC +10216, α Ori, o Ceti, NML Cyg, and NML Tau. Related observations using non-redundant aperture masking techniques have been performed at the Keck I telescope in the near-infrared. Preliminary results at 2.2 μm and 3.1 μm have been obtained on the morphology of the hot dust at the inner radius of the dust formation zone. In some cases (IRC +10216 and VY CMA) a complex morphology has been found. In other cases (NML Tau and NML Cyg) the morphology is more circularly symmetric. Details of our Keck I observations, including preliminary results on stellar diameters at J, H, K, and L, will be presented in the poster paper by Tuthill et al. also at this conference.

1. Introduction

1.1. Infrared Interferometry – A New Tool for Studies of Stellar Environments

Long baseline interferometry has long provided the highest angular resolution available at radio wavelengths, indeed at any wavelength. During the past ten years technical limitations which held back the development of interferometry at optical and infrared wavelengths have been overcome. These include such technologies as the precise measurement and control of distances, which are now routine thanks to Helium-Neon laser interferometers and high precision digital servo control loops. Another key technological development has been that of high quantum efficiency wide bandwidth detectors, such such as avalanche photo-diodes. At the present time several single-baseline interferometers have worked reliably enough that significant observational programs have been undertaken, and as a result of this body of work, there are quite a number of second generation (multiple baseline) interferometers under development, some of which have been recently completed (cf. Danchi & Bester 1995 for a review of interferometers and observational results).

Interferometers are the only tools that stellar astronomers have available with sufficient resolution to *directly* study the environment immmediately surrounding stars other than our own Sun. At 10 μm, for example, the resolution of the Keck telescope is approximately $0\farcs25$, which is five times the angular diameter of the largest stars, approximately $0\farcs050$. Thus, progress on a host of astronomical problems is dependent on interferometric techniques, such as the circumstellar environments of young stellar objects and late stars, both of which have circumstellar dust and gas, and potentially complicated morphologies. Late stars, in particular, have been a choice for much interferometric work in the infrared because they are the largest in angular size and brightest (in apparent magnitude) stars other than the Sun, and because they exhibit mass loss, an important astronomical phenomenon that is not well understood in detail (cf. Lafon & Berruyer 1991 for a recent review).

In this paper we review progress made with the University of California Berkeley Infrared Spatial Inteferometer (ISI) on the distribution of dust surrounding late stars and its implications to mass loss. We begin with a brief historical review of observational work pertaining to mass loss and the importance of interferometry to further progress in the remainder of this Introduction in Section 1. In Section 2 we discuss the instrumentation used by our group: the ISI at 10 μm, and aperture masking in the 1-5 μm region with the Keck telescope. Observational results are discussed in Section 3, a brief summary is presented in Section 4.

1.2. Observational Background

As intermediate mass stars evolve off the main sequence after exhausting their core hydrogen supply, they end up at a stage in which they alternately burn hydrogen and helium in shells surrounding an carbon-oxygen core. Eventually carbon, oxygen, nitrogen and s-process elements are brought to the surface. A star at this stage of evolution is considered to be on the asymptotic giant branch (AGB) of the HR diagram (Iben 1991).

Without the loss of material from stars in winds or mass ejections during the red giant phases, the end state of most intermediate mass stars would be supernovae. Instead, most of these stars are thought to evolve to planetary nebulae after losing much of their mass through a possible assortment of mass loss processes such as cool winds (Salpeter 1974), thermal pulses (Schwarzschild & Harm 1965), and/or other forms of mass ejection.

Mass lost by AGB stars is also important because it contains heavy elements that enrich the interstellar medium. Thus, mass loss is of fundamental importance in understanding the late stages of stellar evolution, particularly the masses and frequencies of white dwarf stars, neutron stars, and black holes. From an observational standpoint, the low frequency of supernovae in the galaxy, which is too low to be accounted for without mass loss, further supports these conclusions. Detailed reviews of mass loss phenomena have been published by Zuckerman (1980), Dupree (1986), Chiosi & Maeder (1986), and by Lafon & Berruyer (1991).

The earliest measurements of mass loss were made by Adams and McCormack (1935) using absorption line spectroscopy of Na I, Ca I (H and K), and Al II. In cool stars these lines show motions of about 5 km s with respect to the stellar photosphere. Deutsch (1956) suggested that mass was actually leaving the Her (M5 I) system at a rate of 3×10^{-8} M yr^{-1}. Dupree et al. (1984) demonstrated that shifts and asymmetries of the absorption cores and line emission wings in H show evidence for expanding cool chromospheres around red giants. Based on the optical and UV measurements, Dupree (1986) noted that mass loss rates increase with decreasing stellar temperature (i.e., later spectral type) and with increasing luminosity. Typical values inferred were 10^{-6} Myr^{-1} for spectral types around M5 and luminosity classes in the range of Ib to II.

Subsequently mass loss rates have been determined by a variety of observational techniques including: (1) fitting emission line profiles of molecules in the envelopes, particularly rotational transitions of carbon monoxide (CO) (cf. Knapp & Morris 1985); (2) fitting mid-infrared spectral emission features (Gillet, Low & Stein 1968; Woolf & Ney 1969; and Gehrz & Woolf 1971; Crabtree & Martin 1979; Rowan-Robinson & Harris 1983; Hashimoto et al. 1990, Skinner & Whitmore 1988); (3) high angular resolution measurements, such as lunar occultation (Toombs et al. 1972), slit-scanned speckle interferometry (Howell et al. 1981), and Michelson stellar interferometry (Sutton et al. 1977, 1979; McCarthy et al. 1977; Danchi et al. 1990; Bester et al. 1991); (4) photometric statistical correlation studies (DeGioia-Eastwood et al. 1981; Jura 1986).

Infrared spectroscopy with high spectral resolution has been used to probe the physical conditions and kinematics of the gas in circumstellar envelopes, such as using fundamental and first overtone CO vibration-rotation spectra at 5 μm and 2 μm (Hinkle, Hall & Ridgway 1982; Keady, Hall, and Ridgway 1988). Evidence for a radial velocity gradient in infrared absorption lines (near 10 m) of silane (SiH_4) and ammonia (NH_3) in the molecular shell around IRC +10216 has been observed by Betz and his collaborators (cf. Betz et al. 1979; Goldhaber & Betz 1984) using infrared heterodyne spectroscopic techniques. Recently, Bowers (1993) has analyzed 22 GHz water masers around a set of Mira and semi-regular variables. His analysis suggests systematic acceleration of the gas occurs outside the SiO maser shell but within a radius of about 10 AU, consistent with the recent results from the ISI.

From a theoretical standpoint, a variety of mechanisms can be found to drive mass loss, such as Alfven waves (Hartmann & McGregor 1980), acoustic waves (Pijpers and Hearn 1989), shock waves (Tuchman et al. 1978; Wood 1979; Willson & Bowen 1986), and probably most commonly studied is dust driving (e.g., Salpeter 1974; Goldreich and Scoville 1976; Tielens 1983). For dust driving theories important issues concern where the dust is condensed, at what temperatures and densities, and if it is consistent with expectations from theories of nucleation and growth of the grains (cf. Draine 1981; Tielens 1990.

1.3. Importance of continued observational work

There now exists a variety of direct and indirect evidence for asymmetries in the dust shells of late type stars. Molecular and polarization data, the fitting of spherically symmetric broad band spectro-photometric models (e.g. Planesas et al. 1990) and VLBI mapping of maser emission (e.g., Greenhill et al. 1995) all suggest departures from symmetry on a number of scales. However, except for one or two nearby examples (e.g., IRC +10216), it has not been possible to image the circumstellar environments of these stars at sufficiently high resolution to infer the details of these asymmetries. Our non-redundant aperture masking program with the Keck I telescope has demonstrated the ability to resolve the hot dust emission on small scales, with preliminary results showing signatures of anisotropic mass-loss close to the stellar surface.

In addition to detecting dust asymmetries, aperture masking data provide information on the stellar surfaces of the target stars at near-infrared wavelengths. Studies at optical wavelengths (Wilson et. al 1992; Tuthill 1994) have revealed large asymmetries in the brightness distributions across the stellar surface, which may be due to the presence of giant convective cells. The ability to detect these features, which becomes possible with 10 m baselines, in the near-infrared will be crucial in constraining their temperatures and sizes, providing the key to their origins and behavior. In addition, there is the possibility of establishing a direct physical link between the photospheric and circumstellar asymmetries, thereby elucidating the role of these features in the mass-loss process itself.

For these stars, an outstanding problem has been the precise determination of their angular diameters (Wood 1990), which has important repercussions for dynamical modeling. Precise diameter measurements coupled with good distance estimates provide the most direct method of determining their mode of stellar pulsation. Interferometric observations at optical wavelengths are problematic because at these wavelengths the stellar spectrum is blanketed and one sees only to intermediate levels in the stellar atmosphere where molecular and atomic species are most populous (Scholz & Takeda 1987).

In summary, high-angular resolution observations in the near- and mid-infrared are of vital importance in advancing our understanding of mass loss, the physical conditions in the extended envelopes of evolved stars, and diameters of these stars. Some of the reasons for this are: (1) dust is expected to condense close to the star; (2) dust emission peaks in the mid-infrared; (3) major observational and theoretical emphasis has been given to the dust driving mechanism of mass loss; (4) the observational literature shows how important infrared observations of dust are as a tracer of mass loss.

2. The Infrared Spatial Interferometer

2.1. Description of Instrument

The Infrared Spatial Interferometer (ISI), constructed for astrometric purposes under the auspices of the Office of Naval Research, consists of two movable telescopes each with 1.65-m aperture. The ISI has been described in several papers (cf. Danchi et al., 1988; Bester et al., 1989, 1990, 1994) and hence it is

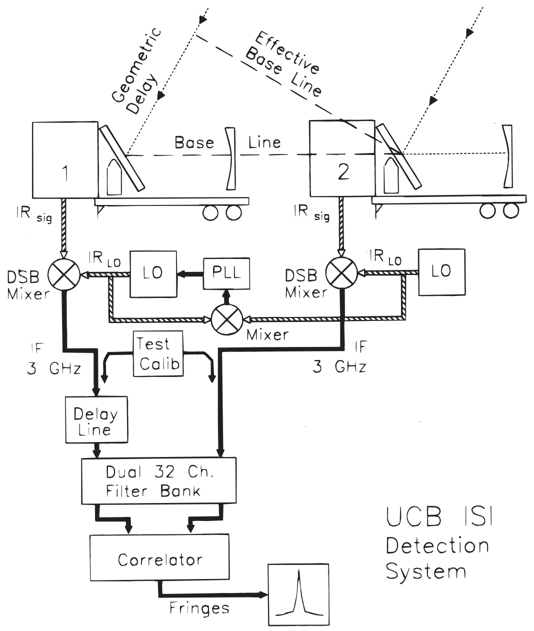

Figure 1. Block diagram of the detection system for the U.C. Berkeley Infrared Spatial Interferometer (ISI), a two-telescope spatial interferometer using heterodyne detection.

discussed only briefly here. Schematics of the system and of one telescope are shown in Figures 1 and 2. The ISI operates in the 9-11 m atmospheric window and is located at Mt. Wilson (1742 m). It comprises two compact, novel-design Pfund telescopes: each telescope consists of a fixed f/3.14 parabolic mirror with 1.65-m aperture and a 2-m diameter flat mirror serving as a coelostat in an alt-az fork mount. To ensure mobility, the large optics and all associated optics and electronics for each telescope are mounted within a standard-size semi-trailer. Critical distances within the telescope optics are monitored with laser metrology, as indicated in Figure 2.

Heterodyne detection is used, with LN cooled HgCdTe photodiodes and phase-locked CO laser local oscillators (LO). The quantum efficiency for heterodyne detection including telescope transmission losses has in the past been about 35%, which corresponds to a system noise temperature of 1860 K (DSB). The IF passband extends from 200 to 2000 MHz. To avoid attenuation by CO in the Earth's atmosphere, the local oscillators are normally operated on CO line.

Heterodyne detection, which responds only to incoming radiation that is coherent over the telescope aperture, and which also has a narrow bandwidth ($\leq$ 6000 MHz for double sideband detection), provides a number of advantages over very wideband direct-detection schemes. These include a rather sure measure of visibility as noted above, simplification of delay lines, an easy extension of the system to many telescopes with no resulting loss of signal-to-noise ratio in any pair, and a natural extension of interferometry to spectral line observations since the bandwidth is comparable with spectral line-widths. However, hetero-

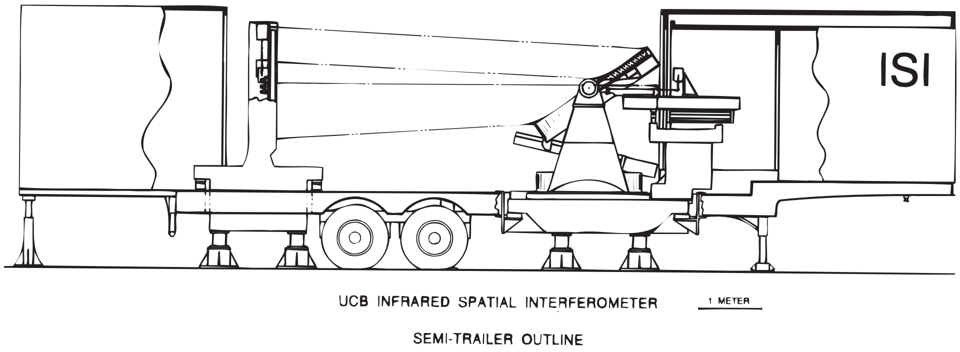

Figure 2. Schematic of one of the Pfund telescopes of the ISI. An 80 inch flat mirror on an alt-az mount acts as a coelostat and sends radiation from an astronomical source to a 65 inch parabola shown on the left. The parabola focuses the radiation through a hole in the flat mirror to the detection system. Each mirror mount stands on a 3 legged kinematic mount independent of the trailer when the telescope is not moved. Dashed lines represent HeNe laser interferometer beams used to monitor distances.

dyne detection has a disadvantage in giving poorer signal-to-noise ratio than does broad-band direct infrared detection (e.g., broad-band photon counting). Theoretical estimates of signal-to-noise by Townes (1984) suggest useful fringe signals could be obtained on stellar sources with intensity greater than about 50 Jy, 5 or 6 magnitudes weaker than the strongest sources such as α Ori.

A number of scientific programs are currently underway. Emphasis is given to studies of the structure of dust shells surrounding late-type stars and also their stellar diameters (e.g., Danchi et al. 1990; Bester et al. 1991; Danchi et al. 1994a), the distribution and excitation of molecules surrounding such stars (cf. Bester et al. 1994), the study of refractivity fluctuations in the atmosphere from turbulence, both near the ground and in the upper atmosphere (Bester et al. 1992, 1994; Treuhaft et al. 1995), and astrometry (Treuhaft et al. 1994).

2.2. A Third Telescope for the ISI

Currently our group is fabricating a third ISI telescope identical to the initial two funded by a grant from the National Science Foundation. This third telescope will allow for observations with three simultaneous baselines and in addition, a closure phase. This development will be a major advance in the field of long baseline interferometry in the mid-infrared since it will provide the first Very Long Baseline Interferometer (VLBI) type imaging in this spectral region. This telescope is expected to be completed in the fall of 1998, and integration and commission of the complete three telescope system will be in the winter of 1998 and the first half of 1999.

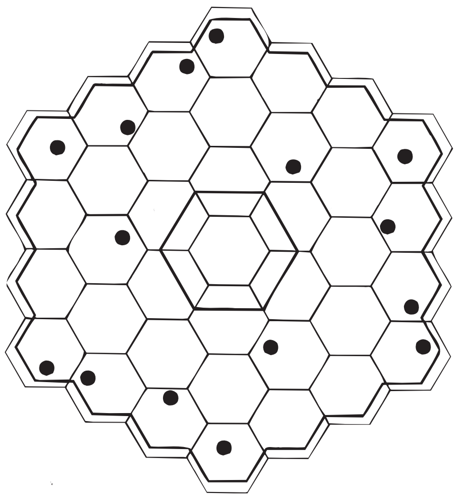

Figure 3. Schematic illustration of 15-hole Golay mask projected on to the primary mirror of the Keck I telescope.

2.3. Non-redundant Aperture Masking in the Near-Infrared at the Keck Observatory

The other major technique used in our high-angular resolution program is that of non-redundant aperture masking on a large telescope, namely the Keck telescope, at approximately J, H, K, and L, photometric bands. This technique was developed in Cambridge, U.K. and provides diffraction-limited imaging interferometrically by masking the pupil in a non-redundant manner, and hence making the telescope into an aperture synthesis interferometer with a large number of baselines. During this past year we were able to reconstruct quite strikingly detailed images of a number of late-stars at 2.2 and 3.1 μm using a 15-hole Golay mask (105 baselines). A schematic of the mask is shown in Figure 3, projected onto the primary mirror of the Keck I telescope.

3. Highlights of Recent Observational Results

3.1. General Considerations

The ISI is being intensively used for observations of circumstellar material around late-type stars (cf. Danchi et al. 1990, Bester et al. 1991, Danchi et al. 1994a, etc.), stellar diameters (Danchi et al. 1994b), refractivity fluctuations of the atmosphere (Bester et al. 1992, 1994, Treuhaft et al. 1995), and wide-angle astrometry (Treuhaft et al. 1994). The present program stars consist of approximately 23 evolved stars that are all bright IRAS 12 μm sources. Some are well-known oxygen-rich supergiant stars such as α Ori or α Sco. Others are classic Mira variables such as o Cet, IK Tau, R Leo, and a few are carbon stars such as CW Leo (IRC+10216), and RW LMi (CIT 6). Two S stars also have been observed, e.g. χCyg and W Aql. Most target stars were chosen because there was a reasonably good base of knowledge about them from other observations and it was clear that high-angular resolution data from the ISI could provide decisive information regarding the process of dust formation and mass loss.

While the observational program focused primarily on observations with the ISI, important auxiliary observations were made on SiO masers surrounding these stars, using the Very Long Baseline Array (VLBA) in collaboration Dr. L. Greenhill of the Harvard-Smithsonian Center for Astrophysics, mid-infrared spectroscopy (7-13 μm) in collaboration with Dr. T. Geballe of the United Kingdom Infrared Telescope (UKIRT), and most recently aperture masking experiments in the near-infrared - J,H,K, and L - bands using non-redundant and partially redundant aperture masks placed in front of the infrared secondary of the Keck I telescope.

At present we have four epochs of data on a "Snapshot Survey" program for most of the stars on the observing list. These observations were to cover two maxima and two minima for a number of the program stars. For some of the stars we have additional data taken with a sub-array of the VLBA. Using the CGS3 instrument at UKIRT we also now have a set of unique mid-infrared spectra taken every few months during the past 1 1/2 years, which for most stars covers a complete luminosity cycle. Striking variations in the shape of the silicate feature have been observed on a number of these stars.

In the ISI observations described here four baselines were used, from 4 m up to 32 m. The shortest baseline provided an effective resolution of $0\overset{''}{.}25$, better than that provided by the largest conventional telescopes (4 m), and equal to that provided by the Keck telescope (10 m). For a single baseline interferometer, such as the ISI, the measured visibility is a single track in the u-v plane (Thompson et al. 1986). For a source with reflection symmetry, the visibility is real and the phase is constant. Until very recently spherical symmetry has always been assumed so that both fringe phase and baseline orientation could be ignored. In this case a single curve of visibility versus spatial frequency contains all the information. Spherically symmetric radiative transfer models of the dust distribution surrounding the stars were computed and visibility curves were calculated from the models and compared with data. A χ^2 fitting procedure was used to optimize model parameters. Further constraints were obtained from comparisons of calculated and measured source spectra.

The radiative transfer model used for most of the analyses was developed by Wolfire and Cassinelli (1986) and was adapted for dust envelopes surrounding late-type stars. (cf. Danchi et al. 1994a). Briefly, the equations of radiative equilibrium were solved iteratively to find the radial temperature distribution. The calculation spans wavelengths from the Lyman edge to 1000 m and naturally computes the specific intensity as a function of impact parameter (angular distance from center of star) and the spectrum. Dust was assumed to be fully condensed at the inner radius, R_0. Physical and optical characteristics of the dust were assumed to have constant radial dependence. The grain size distribution was assumed to be that of the interstellar medium (Mathis et al. 1977), with minimum radius 0.005 μm and maximum 0.25 μm. The grain composition could be varied from pure silicates, graphites, or amorphous carbon (two phases) to mixtures of any two of the four possibilities. The complex dielectric constants of the silicate and graphite grains were taken from Draine & Lee (1984, 1987) for most of the work discussed here, however we also used constants from David & Papoular (1992) and from (Ossenkopf et al. 1992). The latter gave the best fits to the overall shape of the silicate feature and near-infrared spectrum, as is discussed below in connection with our recent analyses of NML Cyg. Dielectric constants for the two phases of amorphous carbon were from Rouleau & Martin (1991). Efficiencies for scattering and absorption were calculated (based on the complex indices of refraction) for dielectric spheres based on the work of Toon & Ackerman (1981). The fixed inputs to the trial models were the stellar effective temperature, angular radius of the star, dust composition, grain size, and primary beam response. The visibility data were fitted by a χ^2 minimization procedure.

In the following subsections, the results of analyses of are discussed, beginning with the initial survey. It has been interesting to see how much the sources change as a function of time. Some of the observed changes have been quite surprising and striking as discussed below.

3.2. Survey of Characteristics of Dust Shells Surrounding Late-type Stars

A survey of the characteristics of the dust shells of 13 of the 23 program stars was published in Danchi et al. (1994a).This publication was a significant milestone in the study of mass loss as it resulted in the first grouping of different dust shell morphologies with different stellar types. Roughly half of the stars had inner radii many stellar radii from their photospheres. These stars include the M supergiants α Ori, α Sco, α Her, the F supergiant IRC+10420, as well as the S stars χ Cyg and W Aql. For the M supergiants this means a sporadic production of dust with a mean interval 30 years. For the S stars a somewhat shorter interval between episodes of dust emission is indicated, perhaps as short as 20 years. The Mira variables R Leo, o Cet, IK Tau, and carbon star IRC+10216 have dust shells with inner radii less than about 6 stellar radii, indicating an almost continuous production of dust. The supergiants VX Sgr, VY CMa, and NML Cyg and the symbiotic star R Aqr also have inner radii of their dust shells close to their photospheres, indicating a nearly continuous production of dust.

The physical conditions at the inner boundary of the dust shell as well as mass loss rates and total masses of dust and gas shells (within a specified angular radius) were discussed in Danchi et al. (1994a). It was found that the densities of hydrogen at the inner radii were such that if dust nucleated at densities 10^{11} cm^{-3}, then it would form at a distance of 0.8 R_* from the photosphere, in rough agreement with the result of Draine (1981). The mass loss rates reported in Danchi et al. (1994a) obtained from the models were compared with those obtained from measurements of the rotational lines CO and other molecules. Using velocities obtained from these lines, total mass loss rates calculated from ISI models for the dust were in approximate agreement over 4 orders of magnitude (cf. Danchi et al. 1994a, Fig. 29). This result indicates that the velocities of the gas and dust must be very similar in value, and that

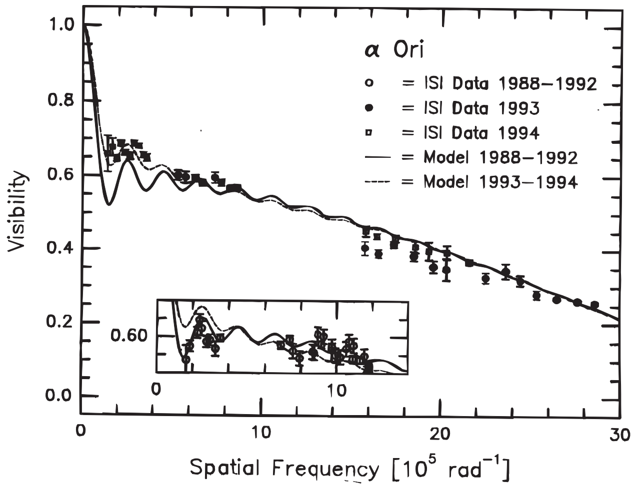

Figure 4. Visibility measurements of α Ori at 11.15 μm taken during 1993-1994, and models to fit these points. For spatial frequencies higher than about 10^5 rad^{-1}, the star is partially resolved.

mass-loss rates may not have changed substantially during approximately the past 100 years.

3.3. Diameters of α Ori and α Sco at 11 μm and a Burst of Recent Dust Formation Around α Ori

An exciting recent result from the ISI concerns measurements of the diameters of stars in the mid-infrared. The longest baseline at present, 32 m, gives sufficiently high resolution that the dust shells around the program stars are resolved, and for the larger stars, the stellar disks themselves are partially resolved. Figure 4 displays visibility data and model curves for α Ori reported in Bester et al. (1996). The angular diameters for the stellar disks of α Ori and α Sco were determined to be 56.6 ± 1 and 44.4 ± 2 mas, respectively, at 11.15 μm. These values are about 10% larger than the most reliable diameters determined at visible wavelengths, and are consistent with predictions of significant optical limb darkening, but only minor infrared limb-darkening. Variations in temperature and luminosity of α Ori during 1989-1995 were studied by interferometry (with the ISI), optical photometry and spectrophotometry leading to the important astrophysical result that observed variations in mare primarily due to temperature changes. A recent episode of dust formation at a distance of 0.1 from the stars was also detected, as can be seen from the change in the observed visibilities (1988-1992) between the solid curve fitting the earlier data and the dashed line representing a model with a thin shell of dust at $0''.1$ in addition to the $1''$ shell previously indicated. This has been identified as due to a discrete mass-loss event of modest size in 1994.

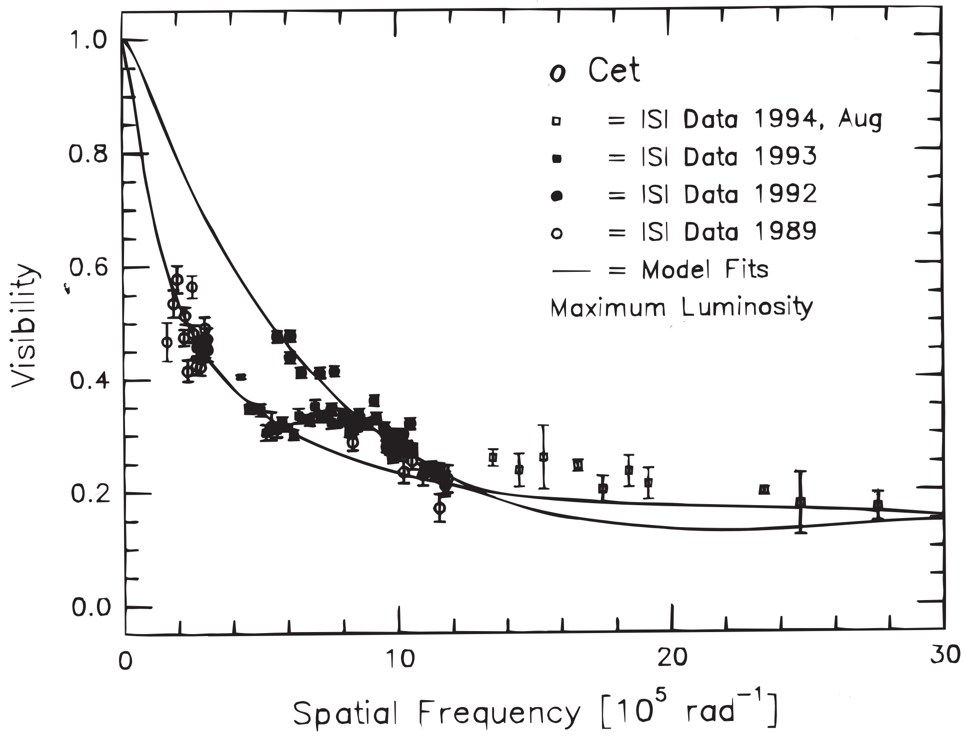

Figure 5. Visibility data and radiative transfer models for o Ceti.

3.4. Non-spherical Structures and Temporal Variations in o Ceti

For some stars, such as o Cet, we have obtained data covering the entire time period from 1988 to 1995 during which the ISI has been in operation. Evidence for dramatic changes in observed visibilities is shown in Figure 5 . Clearly there is a large difference in observed visibilities between 1992 and both before and after as can be seen at spatial frequencies near 6×10^5 rad^{-1}. Analyses of these data are reported in Lopez et al. (1997). For o Cet the observed visibilities change dramatically from one epoch to another and are not consistent with simple heating or cooling of the dust with changes in luminosity phase.

Instead, large temporal variations in density of dust within a few stellar radii of the photosphere are required to explain the data. Spherically symmetric models with two dust shells can explain the variation. But there must be a variation of the density of dust in a shell at 3 stellar radii to fit the observed changes in visibility; not only dust formation, but also destruction is required. Axially symmetric radiative transfer models were also compared with the data, and the radiative transfer method is described in Lopez et al. (1994). Four types of such models were studied-a spherical shell with an inner ellipsoidal cavity, a disk, a spherical shell with one or two inhomogeneities or clumps, and a set of thin partial shells with a fixed distance between them. Of the four models only the one with an inner cavity was excluded. The data were best fitted by model(s) which emphasized inhomogeneities or clumps.

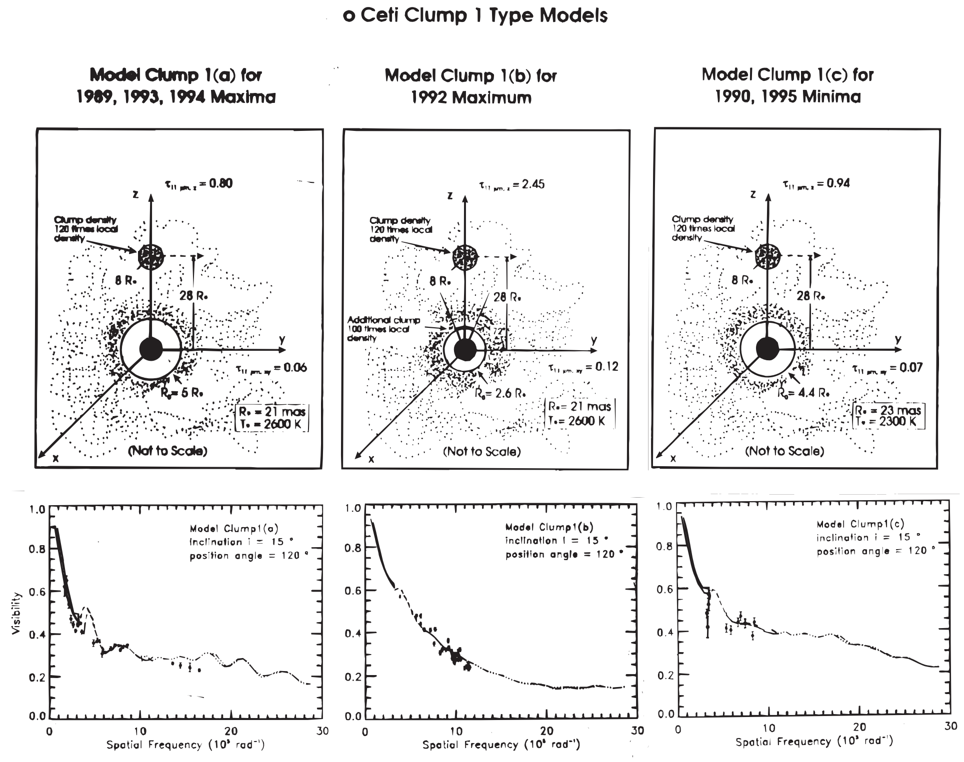

Figure 6. Upper panels display a sequence of models for o Cet beginning with the most recent epoch [Clump 1(a)]. The model Clump 1(b) is derived from Clump 1(a) by the addition of a clump close to the star, partially obscuring the original clump. Clump 1(c) is derived from Clump 1(b) by the removal of the additional clump close to the star. The lower panels display the visibility data and model curves derived from the corresponding clump models on the left hand side, respectively.

Figure 6 displays a sequence of models which are favored at present together with fits to ISI visibility measurements. The success hints at the promise of what detail may be recovered from a complex, asymmetric time variable system by way of our interferometric work. Clearly the combination of geometry and changes in density can account for the observations.

3.5. Non-uniform Outflow from NML Cyg

A dramatic double-shell structure has been detected around NML Cyg. Figure 7 , from Monnier et al. (1997) displays 11 μm visibilities and a maximum entropy method (MEM) fit to the data for NML Cyg, revealing two dust shells, one with maximum annular flux at a radius of 80 mas, the other peaking at 330 mas (solid line). Spherically symmetric radiative transfer models corresponding to this reconstruction are within a continuous outflow shown by the dashed and dot-dashed lines for a thin exponential and Gaussian shell and two Gaussian shells respectively. Note the data are not consistent with a single shell with an inner radius of 40 mas and embedded within a continuous outflow (cf. Ridgway et al. 1986).

This new model for NML Cyg is exciting because it can account for all of the available near- and mid-infrared interferometry data as well as broad-band

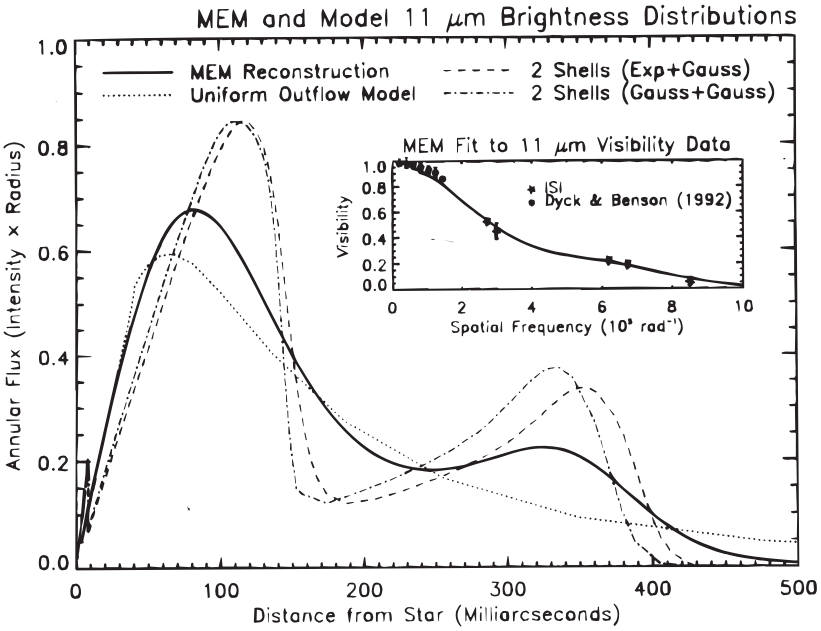

Figure 7. Maximum entropy method (MEM) and radiative transfer model brightness distributions for NML Cyg Inset displays the MEM model fit to the 11 um visibility data.

spectra.. The present models for NML Cyg depart from previously published models (Danchi et al. 1994) in that they utilize the recently published optical constants for silicate dust recommended by Ossenkopf et al. (1992) rather than the classic Draine & Lee (1984, 1987) optical constants. After these models were developed we learned that the locations of the dust shells indicated by the models are at the same locations as the H_20 masers discussed in the paper by Richards et al. (1996). This paper describes maser emission in an approximately circular shell at 100 mas from the center of the star and two blobs of emission 300 mas from the star, one to the northeast, the other to the southwest. Proper motions of the maser features showed that the inner shell is in the zone of acceleration of the outflow, while the masers further out are near the terminal velocity of the outflow, in agreement with expectations based on Danchi et al. (1994a).

Note that the second dust shell at 300 mas was not indicated by prior measurements in the near-infrared. This is due to the fact that the material at this distance from the star is too cool (400 K) to emit strongly in the near-infrared. Interestingly, there are enough adjustable parameters in single shell models to fit virtually all the data except the 11 m visibilities, which could not be fitted by, and hence ruled out, such a model. Thus, mid-infrared interferometry can play a unique role in constraining models of circumstellar dust shells.

3.6. SiO Masers and the Dust Shell of VX Sgr

As mentioned previously observations of SiO masers surrounding our program stars have been an important auxiliary component of the observing program. Observations completed include an initial survey of v=1,2,3 ^{28}SiO and v=0,

^{29}SiO (J=1-0) masers surrounding VX Sgr, Cyg, R Leo, R Cas, W Hya, and VY CMa using a six element subarray of the Very Long Baseline Array (VLBA). Fringes were obtained from baselines as long as 1500 km. The experiment was designed so that emission from all four transitions could be phase-referenced to a common emission feature in the v=2 spectrum providing relative positions to 1 AU free from atmospheric fluctuations. The purpose of the survey was to address the following key issues: 1) temperature and density structure of dust free region; 2) maser pump mechanics of the ^{28}SiO and ^{29}SiO masers; and 3) location of maser emission with respect to the infrared dust emission.

For VX Sgr the SiO maser data from the initial survey was analyzed and published in Greenhill et al. (1994, 1995). This indicated the maser emission was in a ring-like distribution at 1.3 R_* was asymmetric, with the strongest emission to the south of the star. The maser features were consistent with the outflow (or infall) of material away from (or toward) the star of about 10 km sat 1.3 R_*, about 1/2 the velocity of the OH and H_2O maser shells at radii 30 R_*. The maser emission was found to lie well within the 4.6 R_* inner radius of the dust shell, and the stellar diameter was estimated from the ISI visibility data to be 13 $\pm$ 2 mas. The estimated density at the inner edge of the dust shell, location of the masers, and the density at which the maser levels probably thermalize are consistent with models of atmospheric extension due to pulsation driven shocks.

3.7. Recent non-redundant aperture masking results

By utilizing aperture synthesis interferometry techniques at the Keck observatory, we have been able to make images of our program stars at unprecedented angular resolution in the near-IR. We have revealed spectacular and complex morphologies for the hot inner dusty envelopes, showing that the process of mass loss can be far from the simple, spherically symmetric process once believed. Figure 8 displays a map of IRC +10216 at 2.2 microns which gives clear confirmation of flows and clumps in the circumstellar environment. Additional maps have been made in other near-IR bands, allowing estimates of the thermal and optical depth properties of the dust. In order to maximize the scientific insight provided by such maps, it is valuable to compare them with data from polarimetry, maser studies and other high-resolution imaging.

An example of this is provided by VY CMa, where the location of the dramatic one-sided thermal emission seen with Keck interferometry (Figure 9) is found to agree with the location of an extended (3 arcsec) scattering plume seen at 1.25 microns in adaptive optics images from La Silla. Such correlations lend support to the view that mass loss can be highly asymmetric and with preferred directions which are stable over long periods.

3.8. Importance of Correlation Studies

Finally, it is important to analyze and correlate with other observations, particularly our SiO maser data. An example of how interesting such correlations will is illustrated by Figure 10, from Miyoshi et al. (1994), which shows the integrated SiO maser emission for VY CMa. The upper panel is for the v=1 transition; the lower panel for the v=2 transition, which correspond to higher excitation temperatures. The convolving beam is 2 mas (FWHM), although the

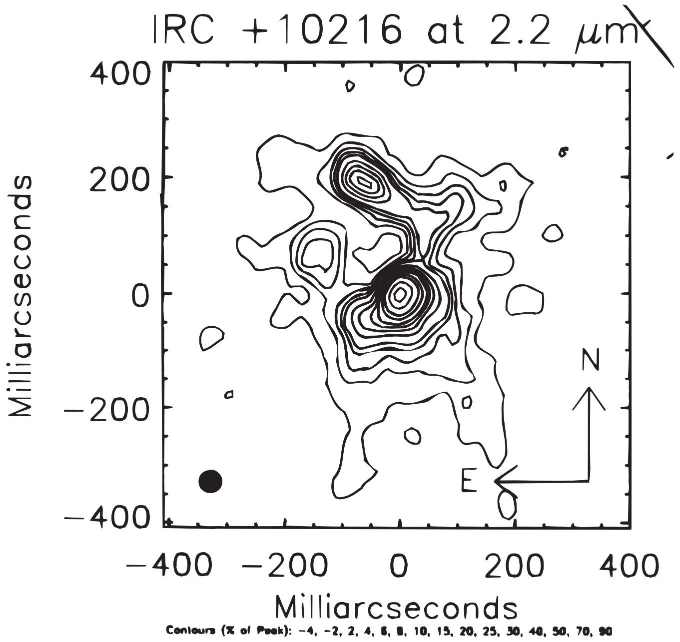

Figure 8. Image of IRC +10216 from the Keck telescope at 2.2 μm using a 15 hole aperture mask.

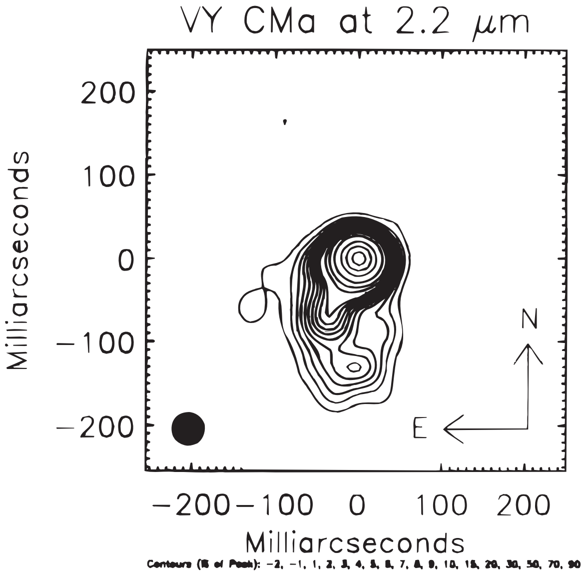

Figure 9. Map of VY CMa at 2.2 μm reconstructed from 15 hole non-redundant aperture mask.

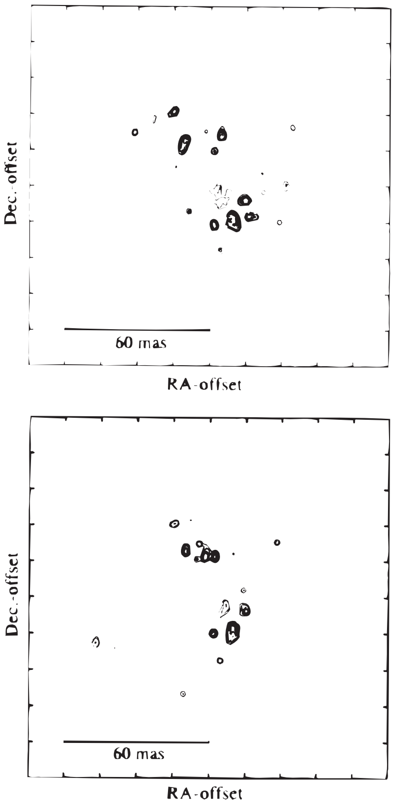

Figure 10. SiO maser maps from Miyoshi et al. (1994) for VY CMa. Upper and lower panels are the v=1 and the v=2 transition, respectively.

synthesized beam is 3 $\times$ 12 mas, elongated north-south. Our own VLBA data set should have an order of magnitude improvement in both sensitivity and dynamic range. It is interesting that the maser spots are essentially anti-correlated with the dust, i.e., the hot dust appears to the south of the star and to the south southwest, while the maser spots are in two clumps, one to the north, the other to the west southwest of the star. There is no simple theoretical explanation for this observation. The present picture is that the SiO masers are in the extended atmosphere, but located inside the dust shell. This may still be true, in that we cannot rule out optically thin dust emission that is not seen in the 2 μm maps (the dynamic range is 100:1). Further observations at 10 m are needed for this, and analysis of more stars is needed to see if this result holds up. It is also unclear as to whether several types of mass loss can be present simultaneously, for example, low-mass spherical outflow related to pulsations, while dense clumps may be emitted sporadically related somehow to surface phenomena.

4. Summary

Our view of the circumstellar environment surrounding evolved stars is changing dramatically as a result of detailed observations performed with long baseline interferometry at mid- and near-infrared wavelengths. Initially mass loss was viewed as largely a quiescent steady state process in a spherically symmetric outflow. At the present time it is clear that: (1) mass loss is sporadic with time scales depending on the spectral and luminosity classes of the stars; (2) the morphology of the dust close to the stellar surface can vary from basically circularly symmetric to rather clumpy with no obvious symmetry, or even to a one sided jet; (3) the effects of binarity need further study. For one widely separated binary system, *o* Ceti, the observed clumpiness is correlated with the location of and direction to the companion; (4) it is interesting to look further at correlations between SiO maser spots and the location of hot dust clumps. At least for one star, VY CMa, they appear to be anti-correlated. The next few years hold great promise for developing a detailed understanding of mass loss, particulary since the new interferometers will allow for complex two-dimensional maps to be made.

Acknowledgments. This work has been supported in part by grants from the National Science Foundation and the Office of the Chief of Naval Research. We have benefitted from fruitful collaborations with Drs. Chris Haniff, T. Geballe, L. Greenhill, B. Lopez, & D. Mekarnia, on part of this work.

References

Adams, W.S. & McCormack, E. 1935, ApJ,81, 119.

Bester ,M., Danchi, W.C., McCullough, P. R. & Townes, C. H. 1989, Lecture Notes in Physics, 331, 296.

Bester, M., Danchi, W.C. & Townes, C.H. 1990, Proc. SPIE, 1237, 40.

Bester, M., Danchi, W.C., Degiacomi, C.G., Townes, C.H. & Geballe, T.R. 1991, ApJ, 367, L27.

Bester, M., Danchi, W.C., Degiacomi, C.G., Greenhill, L.J. & Townes, C.H. 1992, ApJ, 392, 357.

Bester, M., Danchi, W.C., Degiacomi, C.G. & Bratt, P.R. 1994, in Amplitude and Intensity Interferometry II, J.B. Breckinridge (ed.), Proc. SPIE, 2200, 274.

Bester, M., Danchi, W.C., Hale, D., Townes, C.H., Degiacomi, C.G., Mekarnia, D. & Geballe, T.R. 1996, ApJ, 463, 336.

Betz, A.L., McLaren, R.A. & Spears, D.L. 1979, ApJ 229, L97.

Bowers, P.F.1993, in "Sub-arcsecond Radio Astronomy" (eds.) R.J. Davis & R.S. Booth (New York: Cambridge University Press).

Chiosi, C. & Maeder, A. 1986, ARA&A, 24, 329.

Crabtree, D.R. & Martin, P.G. 1979, ApJ, 227, 900.

Danchi, W.C., Bester, M. & Townes, C. H. 1988, in High Resolution Imaging by Interferometry, F. Merkle (ed.), ESO Conference and Workshop Proceedings, 29, 867.

Danchi, W.C., Bester, M., Degiacomi, C.G., McCullough, P.R. & Townes, C.H. 1990, ApJ, 359, L59.

Danchi, W.C., Bester, M., Degiacomi, C.G., Greenhill, L.J. & Townes, C.H., 1994a, AJ, 107, 1469.

Danchi, W.C., & Bester, M. 1995, Ap&SS, 224, 339.

David, P. & Papoular, R. 1992, A&A, 265, 195.

DeGioia-Eastwood, K., Hackwell, J.A., Grasdalen, G.L. & Gehrz, R.D. 1981, ApJ, 245, L75.

Deutsch, A.J., 1956, ApJ, 123, 210.

Draine, B.T. 1981, in Physical Processes in Red Giants, I. Iben & A. Renzini (eds.), (Reidel, Dordrecht), 317.

Draine, B.T. & Lee, T. 1984, ApJ, 285, 89.

Dupree, A.K. Hartmann, L. & Avrett, E.H. 1984, ApJ, 281, L37.

Dupree, A.K. 1986, ARA&A, 24, 377.

Gehrz, R.D. & Woolf, N.J., 1971, ApJ, 165, 285.

Gillet, F., Low, F.J. & Stein, W.A. 1968, ApJ, 154, 677.

Goldhaber, D.M. & Betz, A.L. 1984, ApJ, 279, L55.

Goldhaber, D.M. 1988, Ph.D. Thesis, University of California at Berkeley, unpublished.

Goldreich, P. & Scoville, N. 1976, ApJ, 205, 144.

Greenhill, L.J., Colomer, F., Moran, J.M., Backer, D.C., Danchi, W.C. & Bester, M. 1995, ApJ, 449, 365.

Hartmann, L. & McGregor, K.B. 1980, ApJ 242, 260.

Hashimoto, O., Nakada, Y., Onaka, T., Tanabe, Y. & Kamijo, P. 1990, A&A, 227, 465.

Hinkle, K.H., Hall, D.N.B. & Ridgway, S.T. 1982, ApJ, 252, 697.

Howell R.R, McCarthy D.W. & Low F.J. 1981, ApJ 251, L231.

Iben, I. 1991, ApJSS, 76, 55.

Jura, M. 1986, ApJ, 303, 327.

Karovska, M., Nisenson, P., Papaliolios & Boyle, R.P. 1991, ApJ, 374, L51.

Keady, J.J., Hall, D.N.B. & Ridgway, S.T. 1988, ApJ, 326, 832.

Knapp, G.R. & Morris M. 1985, ApJ 202, 640.

Lafon, J.P. & Berruyer, N.1991, A&AR, 2, 249.

Lopez, B., Mekarnia, D. & Lefevre, J. 1994, A&A, 296, 752.

Lopez, B., Danchi, W.C., Bester, M., Hale, D.D.S., Lipman, E., Monnier, J., Tuthill, P.G., Townes, C.H., Degiacomi, C.G., Geballe, T.R., Greenhill, L.J., Cruzalebes, P., Lefevre, J., Mekarnia, D., Mattei, J.A. & Nishimoto, D. 1992, submitted to ApJ.

Mathis, J.S., Rumpl, W. & Nordsieck, K.H. 1977, ApJ, 217, 425.

McCarthy, D.W., Low, F.J. & Howell, R.R. 1978, ApJ, 223, L113.

Miyoshi, M., Matsumoto, K., Kameno, S., Takaba, H., Iwata, T. 1994, Nature 371, 395.

Monnier, J.M., W.C. Danchi, M. Bester, C.H. Townes, E.A. Lipman, P.G. Tuthill, T.R. Geballe, & D. Nishimoto, ApJ, 481, 420.

Ossenkopf, V., Henning, T. & Mathis, J.S. 1992, A&A, 261, 567.

Pijpers, F.P. & Hearn, A.G. 1989, A&A, 209, 298.

Planesas, P., Kinney J. & Bachiller, R. 1990, ApJ, 364, L9.

Ridgway, S.T., Wells, D. & Joyce, R. 1977, AJ, 82, 414.

Ridgway, S.T., Joyce, R.R., Conners, D., Pipher, J.L. & Dainty, C. 1986, ApJ, 302, 662.

Rouleau, F. & Martin, P.G. 1991, ApJ, 377, 526.

Salpeter, E.E. 1974, ApJ, 193, 585.

Schwarzschild, M. & Harm, R. 1965, ApJ, 142, 855.

Scholz, M. & Takeda, Y. 1987, 186, 200.

Skinner, C.J. & Whitmore, B. 1988, MNRAS, 224, 335.

Sutton, E.C., Storey, J.W.V., Townes, C.H. & Spears, D.L. 1977, ApJ 217,L97.

Sutton, E.C., Betz, A.L., Storey, J.W.V. & Spears, D.L. 1979, ApJ 230, L105.

Tielens, A.G.G.M. 1983, ApJ, 271, 702.

Tielens, A.G.G.M. 1990, in From Miras to Planetary Nebulae: Which Path for Stellar Evolution?, M.O. Mennessier & A. Omont (eds.) (Gif Sur Yvette: Editions Frontieres).

Toombs, R.I., Becklin, E.E., Frogel, J.A., Law, S.K., Porter, F.C. & Westphal, J.A. 1972, ApJ, 173, L71.

Toon, O.B. & Ackerman, T.P. 1981, Appl. Optics, 20, 3657.

Townes, C.H. 1984, J. A&A, 5, 111.

Tuchman, Y., Sack, N. & Barkat, Z. 1978, ApJ, 214, 183.

Treuhaft, R.N., S.T. Lowe, M. Bester, W.C. Danchi & C.H. Townes 1994, in Amplitude and Intensity Interferometry II, J.B. Breckinridge (ed.), Proc. SPIE, 2200, 316.

Treuhaft, R.N., Lowe, S.T., Bester, M., Danchi, W.C. & Townes, C.H. 1995, ApJ, 453, 522.

Tuthill, P.G. 1994, Ph.D. Thesis, Cambridge University, unpublished.

Tuthill, P.G., Monnier, J.M., Danchi, W.C., and Hannif, C. 1997, these proceedins.

Willson, L. & Bowen, G.H. 1986, AJ, 17, 249.

Wilson , R.W., Baldwin J., Buscher D.F. & Warner P.J. 1992, MNRAS 257, 369.

Wolfire, M.G. & Cassinelli, J.P. 1986, ApJ, 310, 207.

Wood, P.R. 1979, ApJ, 190, 609.

Wood, P.R. 1990, in From Miras to Planetary Nebulae: Which Path for Stellar Evolutions?, M.O. Mennessier, A. Omont, (eds.), (Gif sur Yvette, Editions Frontiers), p. 67.

Woolf, N. & Ney, E.P. 1969, ApJ, 155, L181.

Zuckerman, B. 1980, ARA& A, 18, 263.